Predicting Knee Replacement Damage in a Simulator Machine Using a Computational Model With a Consistent Wear Factor

Dong Zhao
Department of Mechanical & Aerospace Engineering,
University of Florida,
Gainesville, FL 32611

Hideyuki Sakoda
Nakashima Medical Division,
Nakashima Propeller Co., Ltd., Japan

W. Gregory Sawyer
Department of Mechanical & Aerospace Engineering,
University of Florida,
Gainesville, FL 32611

Scott A. Banks

Benjamin J. Fregly[1]
e-mail: fregly@ufl.edu

Department of Mechanical & Aerospace Engineering,
Department of Biomedical Engineering,
Department of Orthopaedics and Rehabilitation,
University of Florida,
Gainesville, FL 32611

Wear of ultrahigh molecular weight polyethylene remains a primary factor limiting the longevity of total knee replacements (TKRs). However, wear testing on a simulator machine is time consuming and expensive, making it impractical for iterative design purposes. The objectives of this paper were first, to evaluate whether a computational model using a wear factor consistent with the TKR material pair can predict accurate TKR damage measured in a simulator machine, and second, to investigate how choice of surface evolution method (fixed or variable step) and material model (linear or nonlinear) affect the prediction. An iterative computational damage model was constructed for a commercial knee implant in an AMTI simulator machine. The damage model combined a dynamic contact model with a surface evolution model to predict how wear plus creep progressively alter tibial insert geometry over multiple simulations. The computational framework was validated by predicting wear in a cylinder-on-plate system for which an analytical solution was derived. The implant damage model was evaluated for 5 million cycles of simulated gait using damage measurements made on the same implant in an AMTI machine. Using a pin-on-plate wear factor for the same material pair as the implant, the model predicted tibial insert wear volume to within 2% error and damage depths and areas to within 18% and 10% error, respectively. Choice of material model had little influence, while inclusion of surface evolution affected damage depth and area but not wear volume predictions. Surface evolution method was important only during the initial cycles, where variable step was needed to capture rapid geometry changes due to the creep. Overall, our results indicate that accurate TKR damage predictions can be made with a computational model using a constant wear factor obtained from pin-on-plate tests for the same material pair, and furthermore, that surface evolution method matters only during the initial "break in" period of the simulation.
[DOI: 10.1115/1.2838030]

Keywords: dynamic contact simulation, computational wear prediction, knee simulator machine, total knee replacement, biomechanics

Introduction

Wear of ultrahigh molecular weight polyethylene remains a primary factor limiting the longevity of total knee replacements [1]. Consequently, knee simulator machines are commonly used to evaluate wear performance of new knee implant designs and materials [2–6]. Wear testing on a simulator machine is time consuming and expensive due to the large number of low-frequency cycles that must be run. Moreover, for some machines, different stations sometimes produce different wear results. Consequently, it is impractical to use a knee simulator machine to test the sensitivity of a total knee replacement (TKR) design to the material used, implant geometry, implant alignment, and loading conditions.

Because of these issues, researchers have sought alternative methods to speed up the implant design and evaluation process. Pin-on-plate wear tests [7] using the same material pairs as in a TKR are faster and cheaper to perform than are tests on a knee simulator machine. With a simplified motion path and well-controlled sliding speeds, accurate wear factors can be obtained under test conditions similar to those of knee simulator machines. However, pin-on-plate wear tests do not provide the joint-level damage evaluation desired for design purposes since they do not account for TKR surface geometry or the variety of kinematic conditions occurring across the implant surfaces.

In contrast, computer simulation can be an efficient and reproducible method for predicting TKR wear performance, with simulator machines providing a well-controlled test bed for evaluation. Motion and load inputs are well defined, the number of loading cycles is known precisely, and wear volume can be measured gravimetrically at known intervals for comparison. Though computational damage predictions of TKRs have been developed for the AMTI [8] and Stanmore [9,10] simulator machines, these predictions possess several important limitations. Wear factors were taken from the literature or fine-tuned to match experimental wear volume measurements. Predicted damage depths and areas were not assessed quantitatively. Different types of material models were used in different studies. Finally, apart from Ref. [9], results from a single simulation were extrapolated out to the full number of loading cycles, not accounting for the gradual evolution of the worn surface geometry that occurs in real life. It remains unknown whether a constant wear factor from pin-on-plate tests performed on the same material pair as the implant can be used in a computational damage simulation to predict accurate joint-level damage (depth, area, and volume). Furthermore, how features of

[1]Corresponding author.

Contributed by the Bioengineering Division of ASME for publication in the JOURNAL OF BIOMECHANICAL ENGINEERING. Manuscript received July 31, 2006; final manuscript received May 11, 2007; published online February 5, 2008. Review conducted by Jeffrey A. Weiss.

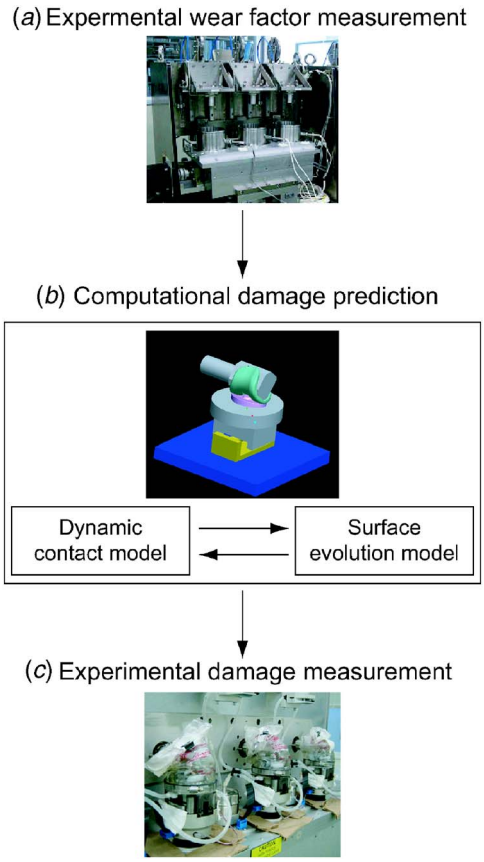

Fig. 1 Overview of the process used to evaluate computational damage predictions for a total knee replacement. (*a*) A constant wear factor is obtained from pin-on-plate experiments using the same material pair as in the implant. (*b*) This wear factor is used in a computational damage prediction that combines a dynamic contact model of the implant in an AMTI simulator machine with a surface evolution model. (*c*) The computational damage predictions are compared to experimental damage measurements made on the same implant during testing in a physical AMTI simulator machine.

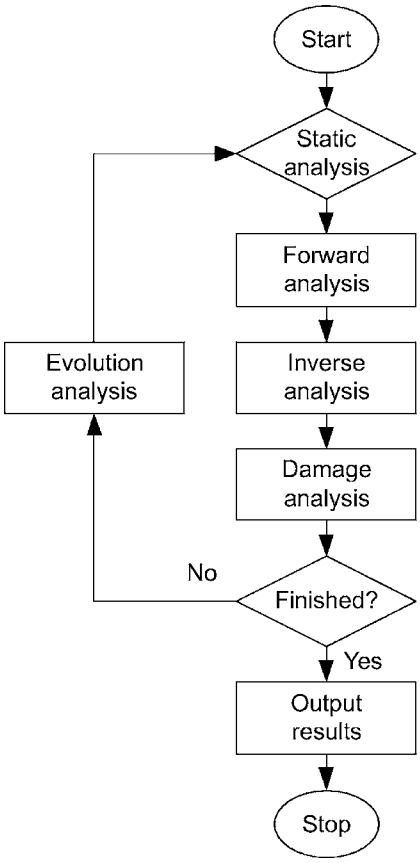

Fig. 2 Flowchart of the iterative series of analyses performed to develop computational damage predictions with surface evolution

the damage model (linear wear plus nonlinear creep) interact with type of surface evolution method (fixed time intervals as in Ref. [9] or variable time intervals) and material model (linear or nonlinear) to affect the damage predictions is also an open issue.

The objectives of this paper were first, to evaluate whether a wear factor from pin-on-plate tests can be used in a computational model to predict accurate joint-level damage in a TKR (Fig. 1), and second, to evaluate how surface evolution method and material model affect the predictions. Two methods for periodically evolving the worn surface geometry are investigated—evolution based on fixed time intervals (i.e., fixed step) and evolution based on a fixed amount of surface change (i.e., variable step). The computational framework is validated analytically using a cylinder-on-plate wear problem with known analytical solution and evaluated experimentally by performing a TKR damage prediction for a commercial knee implant tested in an AMTI simulator machine. The wear factor for the TKR damage prediction is determined experimentally from pin-on-plate tests performed on the same material pair as the implant. Predicted damage depths, damage areas, and wear volumes after 5 million cycles of simulated gait are compared to measurements obtained from the physical simulator machine.

Methods

Computational Framework for Damage Prediction. A computational methodology was developed to simulate progressive surface damage (=wear+creep) over multiple loading cycles. The methodology combines a multibody dynamic contact model with a surface evolution model, where the two models iterate to predict progressive surface damage (Fig. 1(*b*)). The dynamic model was constructed within the PRO/MECHANICA MOTION simulation environment (PTC, Waltham, MA) and incorporated a custom elastic foundation contact model developed specifically for multibody simulations [11]. The dynamic contact model was encapsulated as a dynamic link library using the equations of motion functionality within PRO/MECHANICA MOTION, allowing the model to be incorporated into user-written C++ code. A computational damage model written in C++ was then used to combine the dynamic contact model with a custom surface evolution model, where analyses performed with both models were iterated automatically.

A five-step process was followed to perform computational damage predictions with surface evolution (Fig. 2). The first step was a static analysis to find the initial pose of the contacting bodies prior to performing a forward dynamic simulation. The second step was a forward dynamic simulation (i.e., forward analysis) of the entire system over 1 cycle to predict the relative motion of the contacting bodies at each time instant. The third step was an inverse dynamic analysis to predict contact pressures and sliding conditions on the articulating surfaces at desired time points given the relative motion of the contacting bodies. The fourth step was a damage analysis to calculate the change in damage depth δ_{damage} at each point across the contact surfaces for the specified number of cycles. If the final number of cycles had not been reached, the next step was an evolution analysis to modify

the surface geometry to reflect the total damage depth sustained at each point thus far. Finally, the entire process was iterated, starting with the static analysis, until the specified number of motion cycles had been simulated.

Surface evolution was modeled by using a modified version of an elastic foundation contact model. The traditional elastic foundation model scatters a "bed of springs" over the three-dimensional surfaces to push them apart. The springs represent an elastic layer of known thickness covering one or both bodies, where each spring is independent from its neighbors. For a rigid body contacting a deformable body of finite thickness, a uniform grid of spring "elements" is placed on the deformable body contact surfaces [11], and the contact pressure p for each spring is calculated from [12–14]

$$p = \frac{(1-\nu)E(p)}{(1+\nu)(1-2\nu)}\frac{d}{h} \tag{1}$$

where $E(p)$ is Young's modulus of the elastic layer (a constant for a linear material model and a function of pressure p for a nonlinear material model [15]), ν is Poisson's ratio of the layer, h is the layer thickness at the spring location, and d is the spring deflection, defined as the interpenetration of the undeformed (and unworn) surfaces in the direction of the local surface normal. Both h and d are calculated on an element-by-element basis across the contact surfaces of the deformable body.

The modification to this traditional formulation was to offset the interpenetration d and thickness h of each element by the amount of surface damage δ_{damage} sustained by the element up to the current number of cycles simulated thus far. The modified elastic foundation formula is

$$p = \frac{(1-\nu)E(p)}{(1+\nu)(1-2\nu)}\frac{(d-\delta_{\text{damage}})}{(h-\delta_{\text{damage}})} \tag{2}$$

At the end of each damage analysis, δ_{damage} was calculated on an element-by-element basis and written to a file. At the start of the next iteration, the evolution analysis read in and stored the value of δ_{damage} for each element so that it could be used in the subsequent element pressure calculations. Thus, the interpenetration d between the undeformed contact surfaces continued to be calculated as if no surface damage had occurred.

The calculation of δ_{damage} in the damage analysis accounts for the combined effects of material lost due to mild wear δ_{wear} and surface deformation due to compressive creep δ_{creep}:

$$\delta_{\text{damage}} = \delta_{\text{wear}} + \delta_{\text{creep}} \tag{3}$$

where δ_{wear} and δ_{creep} were calculated separately, allowing wear volume to be calculated separately from total damage volume given knowledge of the area of each element. The total depth of material removed from an element δ_{wear} was predicted using an iterative version of Archard's classic law for mild wear [16]:

$$\delta_{\text{wear}} = \sum_{j=1}^{m} N_j \left(k \sum_{i=1}^{n} p_i |v_i| \Delta t_i \right)_j \tag{4}$$

where i represents time frames within a 1 cycle inverse analysis, n is the total number of time frames in the analysis, j represents an individual inverse anlaysis, m is the total number of inverse analyses performed thus far, and k is a constant wear factor. At any time frame i within a 1 cycle inverse analysis j, p_i is the element contact pressure, $|v_i|$ the magnitude of the element's relative sliding velocity, and Δt_i the time increment used in the analysis, so that $|v_i|\Delta t_i$ represents the sliding distance experienced by the element. For any inverse analysis j, $(k\Sigma_{i=1}^{n} p_i|v_i|\Delta t_i)_j$ is the 1 cycle mild wear depth from Archard's wear law, and N_j is the incremental number of cycles for which the 1 cycle wear depth is to be extrapolated. In practice, only the incremental increase in wear depth $\Delta\delta_{\text{wear}}$ was calculated for the current iteration, and this value was added to the current value of δ_{damage} during the damage analysis.

The total depth of surface deformation on each element due to the compressive creep δ_{creep} was calculated based on curve-fitted UHMWPE creep data reported by Lee and Pienkowski [17–19]:

$$\delta_{\text{creep}} = \left\{ C_1 + C_2 \left[\log\left(\sum_{i=1}^{n} \Delta t_i \cdot \sum_{j=1}^{m} N_j \right) - 4 \right] \right\} \times \frac{\Sigma_{j=1}^{m} N_j \left(\Sigma_{i=1}^{n} p_i / n \right)_j}{\Sigma_{j=1}^{m} N_j} h \tag{5}$$

where $C_1 = 3.491 \times 10^{-3}$ and $C_1 = 7.966 \times 10^{-4}$ are constants and all other quantities are as defined in Eq. (4). The unit for pressure is MPa, the unit for time minutes, and the unit for thickness mm. The quantity $(\Sigma_{i=1}^{n} p_i/n)_j$ is the average pressure on the element over the course of dynamic simulation j, while the quantity $\Sigma_{j=1}^{m} N_j (\Sigma_{i=1}^{n} p_i/n)_j / \Sigma_{j=1}^{m} N_j$ is the average pressure over all cycles N simulated thus far. Unlike the creep model reported in Ref. [20], creep recovery is built into this model since the within-cycle average pressure uses both loaded and unloaded time frames and the between-cycle average pressure accounts for *all* cycles simulated thus far. Unlike for wear, the incremental change (increase or decrease) $\Delta\delta_{\text{creep}}$ in creep could not be calculated directly. Instead, the total amount of creep deformation was calculated from Eq. (5) and the incremental change determined by subtracting the previous value stored in memory. This incremental change was also added to δ_{damage} during the damage analysis.

The calculation of δ_{creep} was complicated by the fact that it relies on past history. To address this issue, we stored the most recent values of $\Sigma_{j=1}^{m} N_j (\Sigma_{i=1}^{n} p_i/n)_j$ and $\Sigma_{j=1}^{m} N_j$ in memory for use during the subsequent damage analysis. Combining these quantities with their incremental changes from the current iteration provided all of the information needed to solve Eq. (5).

The incremental number of cycles N_m at which the contact surface geometry was evolved could be either fixed or variable. Fixed step evolution required a user-defined update interval so that N_m was known in advance. Variable step evolution altered the surface geometry when the calculated surface change ($=\Delta\delta_{\text{wear}} + \Delta\delta_{\text{creep}}$) of any element exceeded a specified threshold value. In this study, we defined this threshold as a specified percentage of the current element thickness $h - \delta_{\text{damage}}$. With this method, the value of N_m required to trigger surface evolution was not known in advance and was found iteratively by solving a nonlinear root-finding problem.

Analytical Validation of Computational Framework. The computational framework was validated by predicting progressive wear in a simple cylinder-on-plate system for which an analytical wear solution was derived. In this system, a rigid cylinder of radius R_c is pressed onto a fixed plate of thickness h and width w by a constant vertical load F_n. The cylinder was considered to be rigid and the plate linearly elastic with Young's modulus E and Poison's ratio υ. The cylinder rotated about its long axis at a constant angular speed S/R_c (i.e., a constant sliding speed of S at each point on the plate surface). Mild wear between the cylinder and plate was described by Archard's wear law using a constant wear factor k. Contact between the cylinder and plate was described by an elastic foundation model. The change in plate thickness due to wear was assumed to be negligible, and the shape of the worn plate surface was assumed to be cylindrical. With these assumptions, we derived analytical solutions (see Appendix for details) for wear volume V_{wear}, maximum wear depth δ_{wear}, and wear area A_{wear} for any number of cycles N:

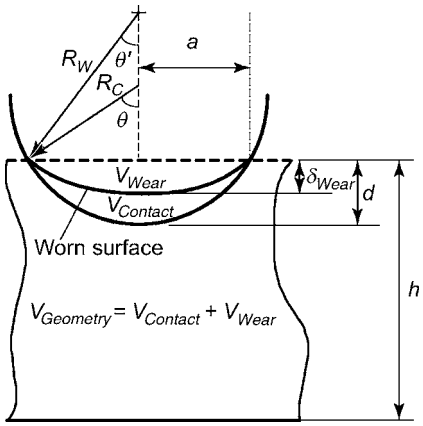

Fig. 3 Schematic of the cylinder-on-plate system used for analytical validation of the computational damage prediction framework

$$V_{\text{wear}} = kNSF_n$$

$$\delta_{\text{wear}} = R_w(1 - \cos\theta') \tag{6}$$

$$A_{\text{wear}} = 2R_c w \sin\theta$$

In these equations, R_w is the radius of the worn surface and θ and θ' are the angles between R_c and R_w, respectively, and a vertical axis (see Fig. 3). The unknowns on the right hand side of Eq. (6) are R_w, θ, and θ'. The derivation produces three coupled nonlinear equations in these three unknowns, which are solved using nonlinear rootfinding methods. Creep is not included in the analytical model since no closed-form solution can be derived in this case.

A computational damage model of the cylinder-plate system was constructed to ensure that the entire framework was working properly as well as to develop empirical rules for fixed and variable step surface evolution. The model was constructed such that the dimensions and material properties of the cylinder and plate were similar to those of a TKR. The cylinder radius was 40 mm and the plate dimensions were 40 mm long by 20 mm wide by 10 mm thick. The cylinder length was 30 mm and the cylinder completely covered the width of the plate. The plate was assumed to be linear elastic with Young's modulus of 463 MPa [21] and Poisson's ratio of 0.46 [22] to emulate polyethylene. The normal force was 1000 N to approximate the maximum load experienced on one condyle during gait. The angular speed of the cylinder was a constant 2π rad/s (60 rpm) corresponding to a 1 Hz frequency. Wear results were generated over 5 million cycles using a constant wear factor of 1×10^{-7} mm^3/N m. The contact element grid density on the plate surface was set to 400×1 where each element had a length of 0.1 mm to span the width of the plate.

The cylinder-on-plate computational model generated wear predictions using fixed and variable step surface evolution with different evolution criteria. The fixed step predictions used criteria of 5, 2.5, 1, 0.5, 0.25, and 0.1 million cycles (mc), while the variable step predictions used criteria of 5%, 2.5%, 1%, 0.5%, 0.25%, and 0.1% of the plate thickness. For both methods, the criterion that produced wear depth, area, and volume errors on the order of 5% at the final time point was selected as the value for use in the subsequent TKR damage predictions.

Experimental Evaluation of Computational Framework. The ultimate goal of the computational framework is to predict surface damage in commercial TKR designs. Thus, to evaluate the framework, we compared computational damage predictions with experimental damage measurements for this situation. Wear testing on an AMTI knee simulator machine was performed on three implants of the same design (Hi-tech Knee II cruciate retaining, Nakashima Medical Division, Nakashima Propeller Co., Ltd., Japan; Fig. 1(*c*)). The machine performed 5 million cycles of simulated gait at a frequency of 1.0 Hz. The lubricant used in the tests was bovine calf serum diluted to 25% with 0.3% sodium azide. The temperature was maintained at 37.0 ± 0.0°C. The tibial inserts were made from GUR 1050 powder by direct compression molding. Before testing, the contact surfaces of one unworn femoral component and tibial insert were digitized using a coordinate measuring machine (CMM) with an accuracy of 0.01 mm. Wear volumes of the three tibial inserts were measured gravimetrically every 1 million cycles, while damage depths and areas for one insert were measured at 5 million cycles using the CMM.

The wear factor for the computational model was obtained by pin-on-plate tests performed with the same material pair used in the implant (Fig. 1(*a*)). In this way, the wear factor used in the computational damage predictions was consistent with the wear tests performed in the simulator machine. The polyethylene pin followed a rectangular wear path of 25 mm by 10 mm. The sliding velocity was 35 mm/s and the total sliding distance was 28 km. The lubricant used in the test was the same as that used in the AMTI machine, and the temperature was maintained at 36.5 ± 1.0°C. The wear factor was calculated based on gravimetrically measured volume loss using a polyethylene density of 0.943 gm/cm^3. The resulting wear factor from three pin-on-plate tests was $2.59\pm0.63\times10^{-7}$ mm^3/N m, with the mean value being used in the TKR computational damage prediction.

A multibody dynamic contact model of one station of an AMTI knee simulator machine was constructed within PRO/MECHANICA MOTION to predict surface damage in the same TKR design (Fig. 1(*b*)). The degrees of freedom in the dynamic model were constructed to match those of the simulator machine, and the implant components were positioned in the model to match their positioning in the physical machine. An additional six degree-of-freedom (DOF) joint between the femoral component and tibial insert was used to measure relative (i.e., joint) kinematics for contact calculations. Each DOF in the model was either motion or load controlled to mimic the function of the AMTI machine. Motion and load inputs to the model were taken as the feedback (i.e., achieved) waveforms measured by the machine during the actual wear tests. Contact surfaces for the femoral component and tibial insert were reverse engineered from the pretest CMM data using Geomagic Studio (Raindrop Geomagic, Research Triangle Park, NC).

Linear and nonlinear material models with Poisson's ratio of 0.46 were used for all damage predictions. The linear model used Young's modulus of 463 MPa. The nonlinear model used a published relationship for the tangent modulus E as a function of contact pressure p [11]:

$$E = 1 \Big/ \left\{ \frac{1}{2}\frac{\varepsilon_o}{p_o}\left[1 + n\left(\frac{p}{p_o}\right)^{n-1} \right] \right\} \tag{7}$$

where $\varepsilon_o=0.0257$, $p_o=15.9$, and $n=3$ are material parameters [23]. Based on computational results for the cylinder-on-plate system, damage predictions with both material models were performed over 5 million cycles of simulated gait using fixed step evolution with an interval of 0.25 million cycles and variable step evolution with a threshold of 0.05%, as well as with no surface evolution.

Results

The wear predictions for the cylinder-on-plate system reproduced the analytical wear results as long as an appropriate surface evolution criterion was used. Wear volume predictions were insensitive to the exclusion or inclusion of surface evolution or to the choice of evolution method, in all cases matching the analytical result to within 0.001% root-mean-square (rms) error after 5 million cycles. In contrast, wear depth and area predictions were highly sensitive to evolution criteria but less sensitive to evolution method (Fig. 4). As the evolution criterion was reduced from 5

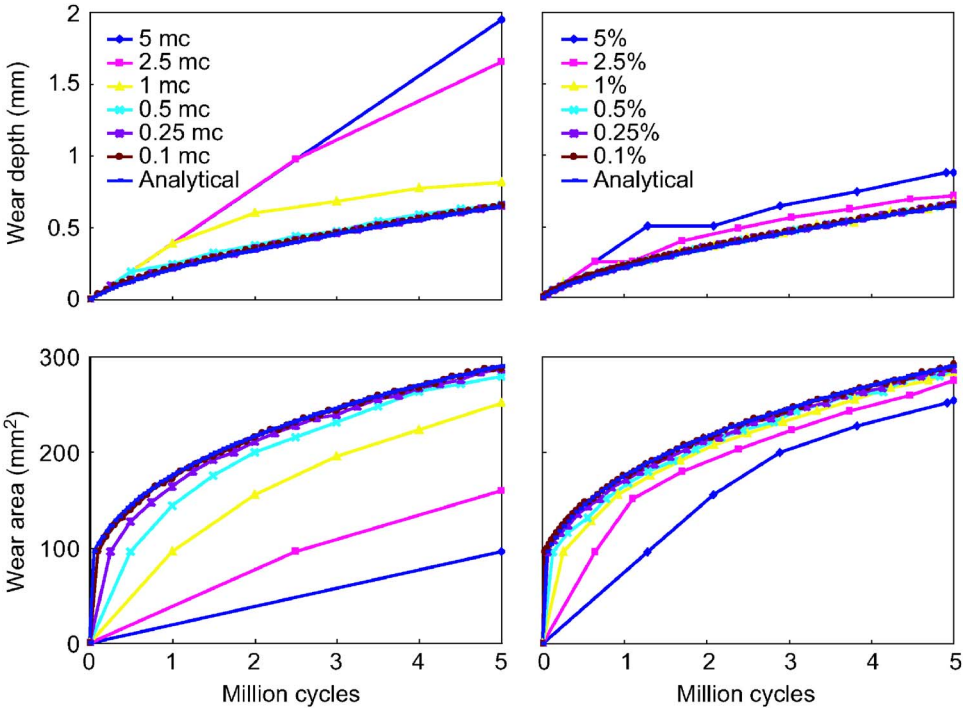

Fig. 4 Comparison of analytical and computational results for wear depth and area for the cylinder-on-plate system. Left column: computational predictions using fixed step surface evolution. Right column: computational predictions using variable step surface evolution.

million cycles or 5%, wear depth and area predictions converged to the analytical solution. When the evolution criterion was too loose, wear depth predictions were too high and wear area predictions were too low with the corresponding wear contours exhibiting unrealistic sharp edges (Fig. 5). Evolution criteria of approximately 0.25 million cycles (fixed step) and 0.05% (variable step) were required to match the analytical damage depth and area to within about 5% rms error (Table 1).

For the TKR system, the computational damage predictions closely matched the experimental damage measurements. Regardless of surface evolution method (none, fixed, or variable) or choice of material model (linear or nonlinear), the predicted wear volume at 5 million cycles was 40.5 mm^3, an error of only 1.5% compared to 39.9 ± 3.4 mm^3 from the three gravimetric wear measurements performed at the end point of each AMTI test (Fig. 6). In contrast, the predicted damage depths and areas were less accurate, with medial-lateral errors of 16% and 18% in damage depth and 10% and less than 1% in damage area (Table 2, nonlinear material model with variable step evolution). Depth and area predictions were insensitive to choice of material model but sensitive to selected evolution method (Fig. 7). No surface evolution resulted in overprediction of damage depth and underprediction of damage area. Only variable step evolution captured a rapid change in surface geometry during the first half-million cycles, with depth predictions for fixed step evolution overshooting the variable step results. Nonetheless, after only 1 million cycles, depth and area predictions from both evolution methods converged to approximately the same trajectory for the remaining 4 million cycles. Fixed step predictions with an evolution criterion of 0.25 million cycles required 20 simulations, while variable step predictions with a threshold of 0.5% required 13 simulations for the linear material model and 11 for the nonlinear model.

The predicted damage regions for the TKR system were in good qualitative agreement with the worn tibial insert obtained from the AMTI machine (Fig. 8). The predicted and measured damage scars were similar in shape and location on the insert, with the predicted locations of maximum damage on the medial and lateral sides being similar to those on the worn insert (x's in Fig. 8). At the anterior-lateral corner of the medial damage scar, a small outcropping region observed experimentally was reproduced by the computational model. Similarly, at the anterior-medial corner of the lateral damage scar, a small incropping region observed experimentally was also reproduced by the model. Switching from the linear to the nonlinear material model or from fixed to variable step evolution had little influence on the predicted damage scars, while switching from no evolution to either evolution method resulted in a noticeable increase in the size of the damage scars (Fig. 9).

Discussion

This study used a computational model to predict damage in a commercial knee implant design after 5 million cycles of simulated gait on an AMTI knee simulator machine. A constant wear factor from pin-on-plate tests performed using the same material pair as in the implant was used to generate the computational predictions. Compared to damage measurements made on the same implant following physical testing on an AMTI machine, wear volumes were predicted to within 2% error, damage depths to within 18% error, and damage areas to within 10% error. Choice of material model (linear versus nonlinear) had little effect on the predictions, while choice of surface evolution method (fixed versus variable) only had an influence during the early cycles (Figs. 7 and 9). In addition to this experimental evaluation, the computational framework was validated using an analytical wear solution derived for a cylinder-on-plate system. Computational damage models may prove valuable in the future for screening new knee implant designs rapidly or performing sensitivity and optimization studies that would be too time consuming or costly to complete with physical simulator machines.

The analytical wear solution for the cylinder-on-plate system permitted an objective evaluation of the proposed computational

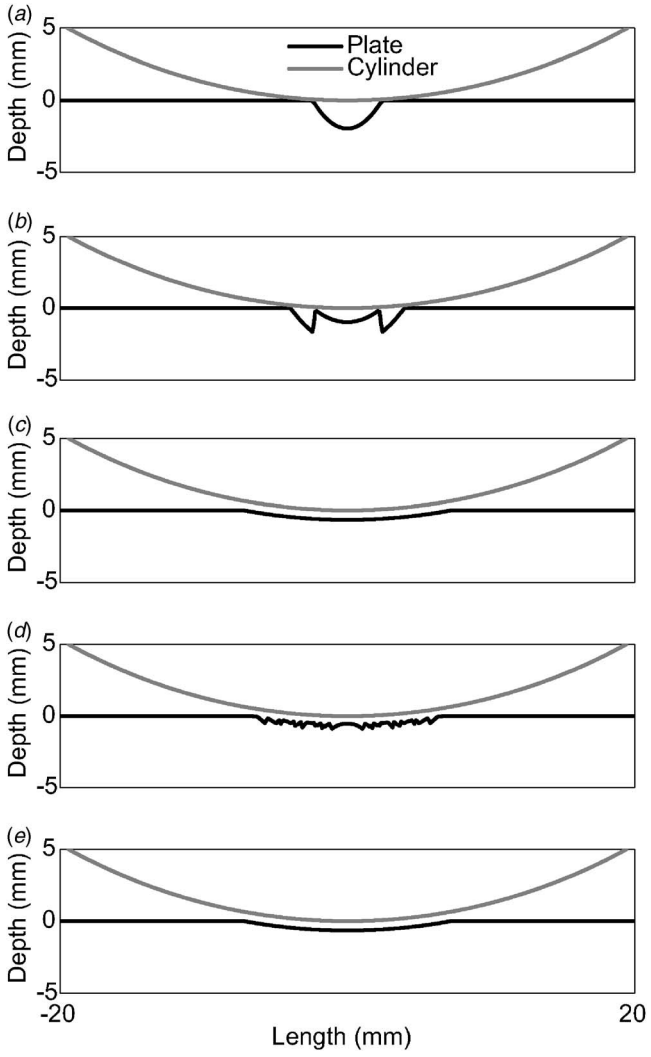

Fig. 5 Cross sectional view of worn plate surface after 5 million cycles (mc) as predicted by the computational damage model using different surface evolution methods and update criteria. (*a*) No evolution (5 mc, 1 simulation), (*b*) fixed step evolution (2.5 mc, 2 simulations), (*c*) fixed step evolution (0.25 mc, 20 simulations), (*d*) variable step evolution (5%, 7 simulations), and (*e*) variable step evolution (0.5%, 19 simulations).

Table 1 Percent rms errors in predicted wear depth, area, and volume after 5 million cycles for the cylinder-on-plate system using fixed and variable step surface evolution with different update criteria. For evolution criterion, mc means millions of cycles and % refers to percent of plate thickness.

Updating method	Evolution criterion	Number of simulations	Wear depth (%)	Wear area (%)	Wear volume (%)
Fixed	5 mc	1	202.2	67.1	0.0
	2.5 mc	2	152.9	51.0	0.0
	1 mc	5	45.9	24.0	0.0
	0.5 mc	10	8.9	10.3	0.0
	0.25 mc	**20**	**2.7**	**4.9**	**0.0**
	0.1 mc	50	2.4	2.1	0.0
Variable	5%	6	42.6	22.1	0.0
	2.5%	8	19.5	13.5	0.0
	1%	13	3.5	7.4	0.0
	0.5%	**18**	**2.6**	**5.1**	**0.0**
	0.25%	28	2.6	3.1	0.0
	0.1%	66	2.6	1.5	0.0

framework with surface evolution. The virtually identical wear volume results for the analytical and numerical models indicated that the numerical computations were being performed correctly. The small error between analytical and numerical wear depth for tight evolution criteria is expected since the worn surface is not a perfect cylinder as assumed in the analytical derivation. The jagged worn surfaces predicted by loose evolution criteria are caused by high contact pressures on the edges of the worn surface from the previous iteration (Figs. 5(*b*) and 5(*d*)). This analytical solution may prove useful as a benchmark test case for other studies performing computational wear prediction.

Identical wear volume predictions with and without surface evolution may have been a consequence of the type of simulator machine and implant geometry used in our study. For the AMTI simulator machine, the anterior-posterior translation and internal-external rotation are motion rather than load controlled. Consequently, for relatively flat tibial insert geometry, as in the current design, the sliding distance on each side was essentially imposed. Even after surface evolution, the tibial surface geometry remained relatively flat. Had the tibial insert geometry been more conformal, wear volume predictions with and without surface updating would likely have been different.

While choice of material model did not have a significant effect on our results, the nonlinear material model was still preferable. It exhibited slightly faster convergence characteristics (i.e., smaller oscillations of damage depth, less underestimation of damage area) compared to the linear material model for a given evolution method and criterion. For example, when we performed additional damage predictions with fixed step evolution using an interval of 1 million cycles, damage depth for the nonlinear material model stopped oscillating by 2 million cycles, while for the linear material it still exhibited small oscillations up to 4 million cycles. These findings are consistent with a previous study that found a 0.5 million cycles fixed step update interval worked well with a nonlinear material model, though no creep model was included [9]. Furthermore, for a given variable step evolution criterion, the nonlinear model required fewer simulations than did the linear material model. Thus, given a choice between the two material models, the nonlinear model appears to be preferable from a computational speed and stability perspective.

Though both fixed step and variable step surface evolution matched the experimental damage results well, variable step evolution is advantageous for two reasons. First, it gives a smoother

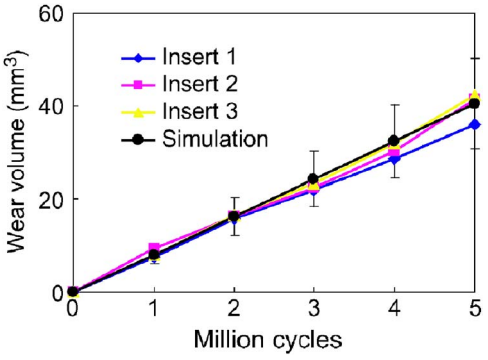

Fig. 6 Comparison of experimentally measured and computationally predicted wear volumes for the knee replacement system over 5 million cycles of simulated gait. Simulation error bars indicate change in predictions due to ±1 standard deviation in wear factor measurement.

Table 2 Quantitative comparison of measured and predicted damage depths and areas for the knee replacement system after 5 million cycles of simulated gait. Experimental measurements were made using a CMM. Computational predictions were generated using variable step surface evolution (0.5% threshold) and the nonlinear material model. Results for other surface evolution and material model combinations were similar (see Figs. 7 and 9).

	Experiment			Simulation		
Damage	Medial	Lateral	Total	Medial	Lateral	Total
Depth (mm)	0.44	0.43	—	0.37	0.35	—
Area (mm^2)	229	212	441	228	233	461

worn surface than does fixed step evolution for the same number of simulations. Second, it can capture rapid changes in surface geometry that cannot be captured by fixed step evolution. In our damage predictions, such rapid changes were caused by our creep model and likely reflect the in vivo situation.

Four modeling assumptions were involved in our TKR damage prediction process. The first was that the elastic foundation contact model is a reasonable approximation of the full three-dimensional elasticity problem. Though this model tends to overestimate contact area and underestimate contact depth, these inaccuracies become even smaller as the worn surface geometry becomes more conformal. As suggested by the quality of our predictions, the elastic foundation model appears to be adequate for predicting knee replacement contact mechanics as long as subsurface stress information is not required. The second assumption was that the surface evolution method only modifies the surfaces in the direction of their original unworn surface normals. As the damage process progresses, the normal direction of each contact element is not adjusted. However, since the damage depths remained "small" after 5 million cycles, and since the damage predictions were in good agreement with experimental observations, the influence of this assumption was likely negligible. The third assumption was that the wear factor used in Archard's wear law was a constant. The literature reports that wear factor measurements can be affected by a number of conditions, such as surface roughness [24], contact pressure [25], lubricant [26], wear path [27], and time-varying loading [25]. Despite these observations, the constant wear factor used in our study, which was not fine-tuned to match the AMTI damage measurements, worked exceptionally well for predicting joint-level wear volume with the computational model. The fourth assumption was that creep deformation after 5 million cycles was not recoverable. By accounting for the time history of loading and unloading, our creep model can reproduce loading and unloading curves reported in the literature [12–14]. If we allowed our creep model to relax for a long enough time, all of the creep deformation would be recovered, since our model calculates creep based on the average pressure over all cycles. Thus, the creep predicted by our model may represent a combination of viscoelastic and plastic effects. If we leave out our creep model, wear volume and damage area are still predicted accurately as long as surface evolution is used, while damage depth is underestimated by approximately 50%. Additional experimental creep data would be needed to refine the current creep model further.

It is not immediately clear why the wear factor measured using the selected rectangular path resulted in accurate wear volume predictions when used in the computational simulations. If we had used a different wear path (e.g., simple linear motion or different rectangular motion), we would have measured a different pin-on-plate wear factor due to a different amount of cross shear [28].

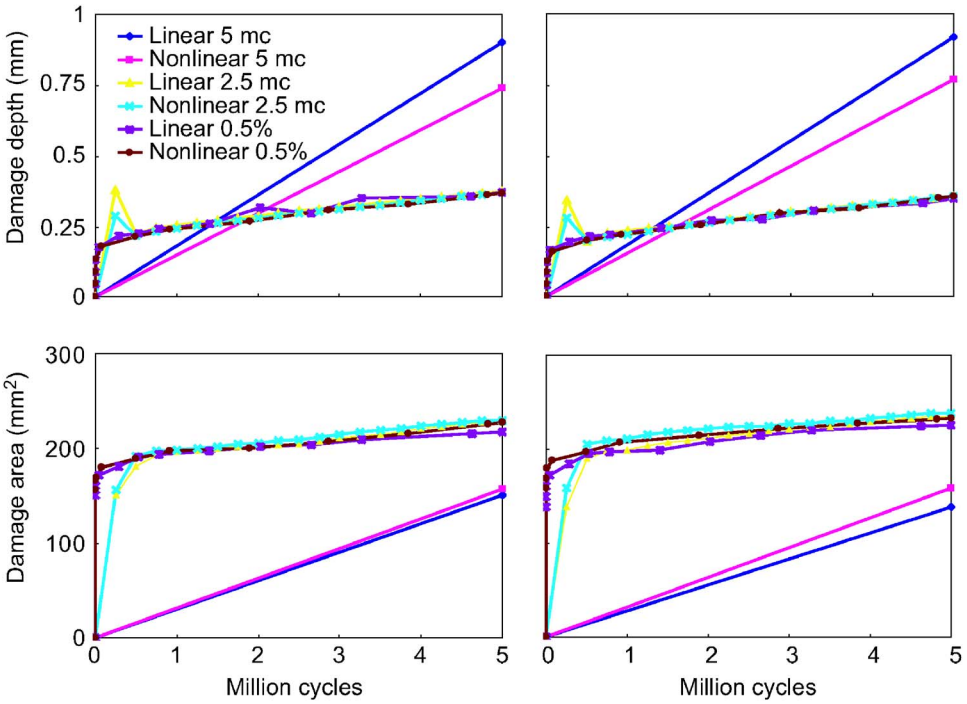

Fig. 7 Damage depth and area predictions for the knee replacement system generated using fixed and variable step surface evolution. Left column: medial side. Right column: lateral side.

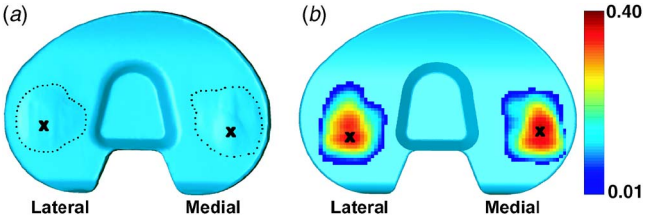

Fig. 8 Qualitative comparison of measured and predicted damage scars after 5 million cycles of simulated gait. (*a*) Experimental damage scars measured by a CMM. (*b*) Computational damage scars predicted using variable step evolution with a threshold of 0.5% and the nonlinear material model. x's indicate locations of maximum damage.

One possible explanation is that the constant wear factor measured by our pin-on-plate tests was consistent with the average cross shear experienced over the tibial insert surfaces. Though different locations on the insert experience different amounts of cross shear [29], a wear factor consistent with the average value may produce joint-level wear volume predictions consistent with the simulator machine results. Another possible explanation is that the experimentally measured wear factor was consistent with the regions on the insert surfaces that experienced the worst cross shear and that these regions dominated the wear volume predictions. A third possible explanation is that the wear factor increases rapidly between a linear motion and one with a small amount of cross shear, changing in a much more gradual fashion with further increases in cross shear. If true, the wear factor may have remained relatively constant for the range of cross shear motions experienced by the insert surfaces.

To investigate how a different wear factor would have changed our computational damage predictions, we repeated our variable step surface evolution simulation with the nonlinear material model using a wear factor that was half the original one. As expected, the predicted wear volume was cut in half. However, the damage areas were reduced by only 6–8% and the damage depths by 17–19%. Thus, the predicted damage areas and depths were much less sensitive to the value of the wear factor than was the predicted wear volume.

The most significant limitation of our study was that only a single implant design and simulator machine were available for analysis. It is difficult to find pin-on-plate wear factor data for the same material pair used in an implant tested on a simulator machine. Furthermore, it is difficult to find experimental data for pin-on-plate and corresponding simulator tests that are performed well. Whether or not the accuracy of our predictions is generalizable to other implant designs and types of simulator machines will require further investigation.

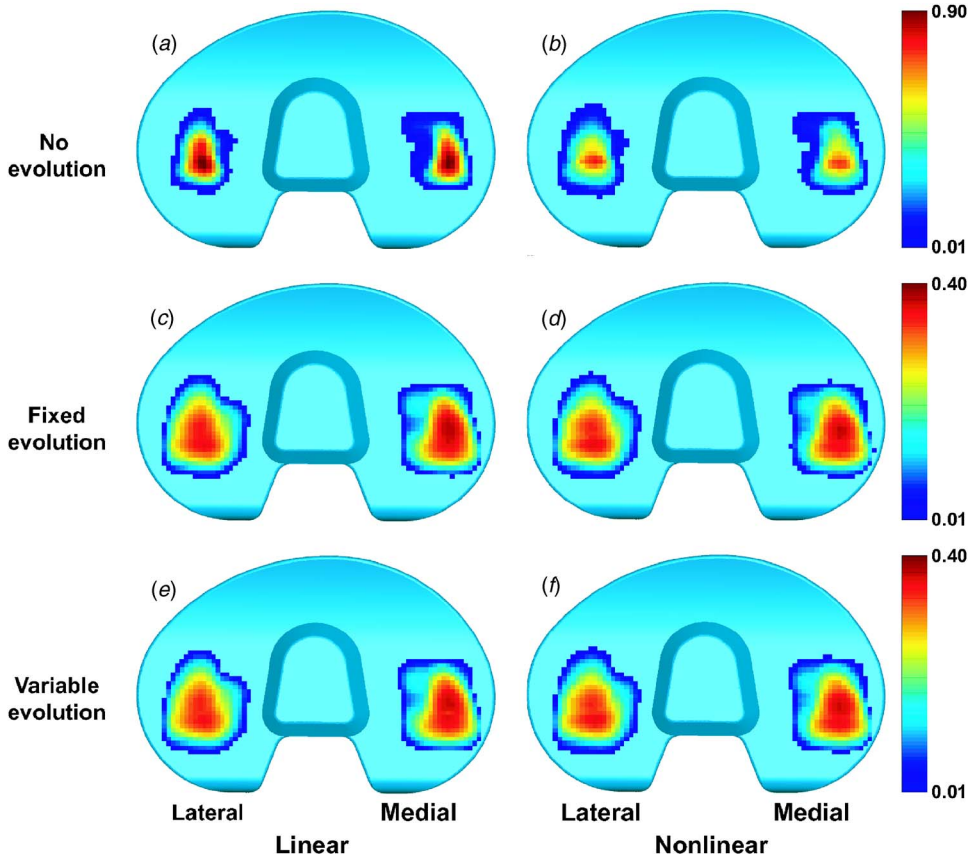

Fig. 9 Qualitative comparison of predicted damage contours for different combinations of surface evolution and material model after 5 million cycles (mc) of simulated gait. (*a*) no evolution with linear material model; (*b*) no evolution with nonlinear material model; (*c*) Fixed step evolution with linear material model (0.25 mc, 20 simulations); (*d*) fixed step evolution with nonlinear material model (0.25 mc, 20 simulations); (*e*) variable step evolution with linear material model (0.5%, 13 simulations); and (*f*) variable step evolution with nonlinear material model (0.5%, 11 simulations).

Acknowledgment

This work was supported by a NSF CAREER award to B.J.F. and by Nakashima Medical Division, Nakashima Propeller Co., Ltd., Japan.

Appendix

An analytical solution for the wear depth δ_{wear}, wear area A_{wear}, and wear volume V_{wear} of a cylinder-on-plate system for any number of cycles N can be derived from geometric relationships along with Archard's wear law and the elastic foundation contact model. The cylinder is treated as rigid with radius R_c and the plate as linearly elastic with constant thickness h and width w. The cylinder rotates about its long axis at a constant angular speed S/R_c so that each location on the plate surface within the contact zone experiences a constant sliding speed S.

An analytical expression for V_{wear} is the easiest equation to derive. If δ_l is the accumulated wear depth at any location l on the plate surface, then wear volume can be found by integrating wear depth across the contact zone:

$$V_{\text{wear}} = \int \delta_l dA \tag{A1}$$

where dA is a differential area. In this equation, δ_l is found from Archard's wear law,

$$\delta_l = k p_l NS \tag{A2}$$

where k is a constant wear factor, p_l is contact pressure, and NS is the total sliding distance over N cycles. Substituting Eq. (A2) into Eq. (A1) produces

$$V_{\text{wear}} = kNS \int p_l dA \tag{A3}$$

Since $\int p_l dA$ is just the normal contact force F_n applied to the cylinder, the wear volume can be expressed concisely as

$$V_{\text{wear}} = kNSF_n \tag{A4}$$

Expressions for δ_{wear} and A_{wear} are more difficult to derive. To perform the derivation, we require two assumptions. First, the change in plate thickness is negligible, and second, the shape of the worn plate surface is cylindrical. Starting from the center of the worn cylindrical surface of unknown radius R_w, δ_{wear} can be expressed as the difference between the distance to the bottom of the worn surface and the distance to the plane:

$$\delta_{\text{wear}} = R_w(1 - \cos\theta') \tag{A5}$$

where θ and θ' are as defined in Fig. 3. In this equation, R_w, θ, and θ' are unknown. Similarly, since contact area for an elastic foundation model is defined using the interpenetration of the undeformed surfaces, A_{wear} can be expressed as

$$A_{\text{wear}} = 2aw = 2R_c \sin\theta w \tag{A6}$$

where θ is again unknown. Thus, a solution for R_w, θ, and θ' is required to solve for δ_{wear} and A_{wear}.

To obtain three equations in the three unknowns R_w, θ, and θ', we use three different geometric relationships. First, we use the fact that the half-width a of the wear zone equals the half-width of the contact zone:

$$a = R_c \sin\theta = R_w \sin\theta' \quad 0 \le a \le R_c \tag{A7}$$

Second, we describe the cylindrical wear volume using a geometric relationship for the intersection area between a circle and line. This area is found by subtracting an isosceles triangle area from a circular sector area (Fig. 3). Multiplying the result by the plate width w produces

$$V_{\text{wear}} = R_w^2(\theta' - \sin\theta'\cos\theta')w \tag{A8}$$

where V_{wear} is known from Eq. (A4). Third, we use the same geometry relationship in conjunction with the elastic foundation model to generate a new expression for F_n. As indicated above, $F_n = \int p_l dA$, where p_l is defined by

$$p_l = \frac{(1-\nu)E}{(1+\nu)(1-2\nu)} \frac{(d_l - \delta_l)}{(h - \delta_l)} \approx C(d_l - \delta_l) \tag{A9}$$

assuming $h \ll \delta_l$. In this equation, d_l is the interpenetration between the unworn surfaces at location l, and C is a constant that accounts for the material properties and thickness of the plate. With this expresson for p_l, the normal force can be written as

$$F_n = C \int (d_l - \delta_l) dA = C(V_{\text{geometry}} - V_{\text{wear}}) \tag{A10}$$

where V_{wear} is known from Eq. (A4) and V_{geometry} is given by an equation similar to Eq. (A8) for the intersection between the cylinder and unworn plane:

$$V_{\text{geometry}} = R_c^2(\theta - \sin\theta\cos\theta)w \tag{A11}$$

Substituting Eqs. (A4) and (A11) into Eq. (A10) yields

$$F_n = C[R_c^2(\theta - \sin\theta\cos\theta)w - kNSF_n] \tag{A12}$$

Thus, Eqs. (A7), (A8), and (A12) provide three nonlinear equations in the three unknowns R_w, θ, and θ', which can be solved for any given number of cycles N using standard nonlinear root-finding methods.

References

[1] Sharkey, P. F., Hozack, W. J., Rothman, R. H., Shastri, S., and Jacoby, S. M., 2002, "Insall Award Paper. Why are Total Knee Arthroplasties Failing Today?" Clin. Orthop. Relat. Res., **404**, pp. 7–13.
[2] Barnett, P. I., McEwen, H. M., Auger, D. D., Stone, M. H., Ingham, E., and Fisher, J., 2002, "Investigation of Wear of Knee Prostheses in a New Displacement/Force-Controlled Simulator," Proc. Inst. Mech. Eng., Part H: J. Eng. Med., **216**, pp. 51–61.
[3] Burgess, I. C., Kolar, M., Cunningham, J. L., and Unsworth, A., 1997, "Development of a Six Station Knee Wear Simulator and Preliminary Wear Results," Proc. Inst. Mech. Eng., Part H: J. Eng. Med., **211**, pp. 37–47.
[4] DesJardins, J. D., Walker, P. S., Haider, H., and Perry, J., 2000, "The Use of a Force-Controlled Dynamic Knee Simulator to Quantify the Mechanical Performance of Total Knee Replacement Designs During Functional Activity," J. Biomech., **33**, pp. 1231–1242.
[5] Muratoglu, O. K., Perinchief, R. S., Bragdon, C. R., O'Connor, D. O., Konrad, R., and Harris, W. H., 2003, "Metrology to Quantify Wear and Creep of Polyethylene Tibial Knee Inserts," Clin. Orthop. Relat. Res., **410**, pp. 155–164.
[6] Walker, P. S., Blunn, G. W., Broome, D. R., Perry, J., Watkins, A., Sathasivam, S., Dewar, M. E., and Paul, J. P., 1997, "A Knee Simulating Machine for Performance Evaluation of Total Knee Replacements," J. Biomech., **30**, pp. 83–89.
[7] Fisher, J., McEwen, H. M., Tipper, J. L., Galvin, A. L., Ingram, J., Kamali, A., Stone, M. H., and Ingham, E., 2004, "Wear, Debris, and Biologic Activity of Cross-Linked Polyethylene in the Knee: Benefits and Potential Concerns," Clin. Orthop. Relat. Res., **428**, pp. 114–119.
[8] Zhao, D., Sawyer, W. G., and Fregly, B. J., 2006, "Computational Wear Prediction of UHMWPE in Knee Replacements," J. ASTM Int., **3**, pp. 45–50.
[9] Knight, L. A., Pal, S., Coleman, J. C., Bronson, F., Haider, H., Levine, D. L., Taylor, M., and Rullkoetter, P. J., 2007, "Comparison of Long-Term Numerical and Experimental Total Knee Replacement Wear During Simulated Gait Loading," J. Biomech., **40**, pp. 1550–1558.
[10] Rawlinson, J. J., Furman, B. D., Li, S., Wright, T. M., and Bartel, D. L., 2006, "Retrieval, Experimental, and Computational Assessment of the Performance of Total Knee Replacements," J. Orthop. Res., **24**, pp. 1384–1394.
[11] Bei, Y., and Fregly, B. J., 2004, "Multibody Dynamic Simulation of Knee Contact Mechanics," Med. Eng. Phys., **26**, pp. 777–789.
[12] Johnson, K. L., 1985, *Contact Mechanics*, Cambridge University Press, Cambridge.
[13] Blankevoort, L., Kuiper, J. H., Huiskes, R., and Grootenboer, H. J., 1991, "Articular Contact in a Three-Dimensional Model of the Knee," J. Biomech., **24**, pp. 1019–1031.
[14] An, K. N., Himeno, S., Tsumura, H., Kawai, T., and Chao, E. Y., 1990, "Pressure Distribution on Articular Surfaces: Application to Joint Stability Evaluation," J. Biomech., **23**, pp. 1013–1020.
[15] Nuno, N., and Ahmed, A. M., 2001, "Sagittal Profile of the Femoral Condyles and Its Application to Femorotibial Contact Analysis," ASME J. Biomech. Eng., **123**, pp. 18–26.
[16] Archard, J. F., and Hirst, W., 1956, "The Wear of Metals Under Unlubricated

Conditions," Proc. R. Soc. London, Ser. A, **236**, pp. 397–410.
[17] Lee, K. Y., and Pienkowski, D., 1997, "Reduction in the Initial Wear of Ultra-high Molecular Weight Polyethylene After Compressive Creep Deformation." Wear, **203-204**, pp. 375–379.
[18] Lee, K. Y., and Pienkowski, D., 1998, "Viscoelastic Recovery of Creep-Deformed Ultra-High Molecular Weight Polyethylene (UHMWPE)," ASTM Spec. Tech. Publ., STP **1307**, pp. 30–36.
[19] Lee, K. Y., and Pienkowski, D., 1998, "Compressive Creep Characteristics of Extruded Ultrahigh-Molecular-Weight Polyethylene," J. Biomed. Mater. Res., **39**, pp. 261–265.
[20] Fregly, B. J., Sawyer, W. G., Harman, M. K., and Banks, S. A., 2005, "Computational Wear Prediction of a Total Knee Replacement From In Vivo Kinematics," J. Biomech., **38**, pp. 305–314.
[21] Kurtz, S. M., Jewett, C. W., Bergstrom, J. S., Foulds, J. R., and Edidin, A. A., 2002, "Miniature Specimen Shear Punch Test for UHMWPE Used in Total Joint Replacements," Biomaterials, **23**, pp. 1907–1919.
[22] Bartel, D. L., Rawlinson, J. J., Burstein, A. H., Ranawat, C. S., and Flynn, W. F., Jr., 1995, "Stresses in Polyethylene Components of Contemporary Total Knee Replacements," Clin. Orthop. Relat. Res., **317**, pp. 76–82.
[23] Fregly, B. J., Bei, Y., and Sylvester, M. E., 2003, "Experimental Evaluation of an Elastic Foundation Model to Predict Contact Pressures in Knee Replacements," J. Biomech., **36**, pp. 1659–1668.
[24] Lancaster, J. G., Dowson, D., Isaac, G. H., and Fisher, J., 1997, "The Wear of Ultra-High Molecular Weight Polyethylene Sliding on Metallic and Ceramic Counterfaces Representative of Current Femoral Surfaces in Joint Replacement," Proc. Inst. Mech. Eng., Part H: J. Eng. Med., **211**, pp. 17–24.
[25] Barbour, P. S., Barton, D. C., and Fisher, J., 1997, "The Influence of Stress Conditions on the Wear of UHMWPE for Total Joint Replacements," J. Mater. Sci.: Mater. Med., **8**, pp. 603–611.
[26] Saikko, V., and Ahlroos, T., 2000, "Wear Simulation of UHMWPE for Total Hip Replacement With a Multidirectional Motion Pin-on-Disk Device: Effects of Counterface Material, Contact Area, and Lubricant," J. Biomed. Mater. Res., **49**, pp. 147–154.
[27] Endo, M. M., Barbour, P. S., Barton, D. C., Wroblewski, B. M., Fisher, J., Tipper, J. L., Ingham, E., and Stone, M. H., 1999, "A Comparison of the Wear and Debris Generation of GUR 1120 (Compression Moulded) and GUR 4150HP (Ram Extruded) Ultra High Molecular Weight Polyethylene," Biomed. Mater. Eng., **9**, pp. 113–124.
[28] Marrs, H., Barton, D. C., Jones, R. A., Ward, I. M., and Fisher, J., 1999, "Comparative Wear Under Four Different Tribological Conditions of Acetylene Enhanced Cross-Linked Ultra High Molecular Weight Polyethylene," J. Mater. Sci.: Mater. Med., **10**, pp. 333–342.
[29] Hamilton, M. A., Sucec, M. C., Fregly, B. J., Banks, S. A., and Sawyer, W. G., 2005, "Quantifying Multidirectional Sliding Motions in Total Knee Replacements," J. Tribol., **127**, pp. 280–286.